Multifractal Structures Detected by *Voyager 1* at the Heliospheric Boundaries

W. M. Macek[1,2], A. Wawrzaszek[2],

and

L. F. Burlaga[3]

Received _____; accepted _____

Submitted to Ap. J. Lett., 15 July 2014, accepted 26 August 2014, published 15 September 2014.

[1]Faculty of Mathematics and Natural Sciences, Cardinal Stefan Wyszyński University, Wóycickiego 1/3, 01-938 Warsaw, Poland

macek@cbk.waw.pl

[2]Space Research Centre, Polish Academy of Sciences, Bartycka 18 A, 00-716 Warszawa, Poland

anna.wawrzaszek@cbk.waw.pl

[3]NASA Goddard Space Flight Center, Code 673, Greenbelt, MD 20771, USA

lburlagahsp@verizon.net

ABSTRACT

To better understand the dynamics of turbulent systems we have proposed a phenomenological model based on a generalized Cantor set with two rescaling and one weight parameters. In this Letter, using recent *Voyager 1* magnetic field data, we extend our two-scale multifractal analysis further in the heliosheath beyond the heliospheric termination shock, and even now near the heliopause, when entering into the interstellar medium for the first time in human history. We have identified the scaling inertial region for magnetized heliospheric plasma between the termination shock and the heliopause. We also show that the degree of multifractality decreases with the heliocentric distance and is still modulated by the phases of the solar cycle in the entire heliosphere including the heliosheath. Moreover, we observe the change of scaling toward a non-intermittent (non-multifractal) behavior in the nearby interstellar medium, just beyond the heliopause. We argue that this loss of multifractal behavior could be a signature of the expected crossing of the heliopause by *Voyager 2* in the near future. The results obtained demonstrate that our phenomenological multifractal model exhibits some properties of intermittent turbulence in the solar system plasmas, and we hope that it could shed light on universal characteristics of turbulence.

Subject headings: ISM: magnetic fields – solar wind – Sun: heliosphere – turbulence

1. Introduction

We have used time series analysis of solar wind plasma with frozen-in magnetic field obtained from various space missions, exploring the inner and outer heliosphere during different phases of solar activity (Macek & Szczepaniak 2008; Macek & Wawrzaszek 2009; Wawrzaszek & Macek 2010; Macek 2012). At present we focus on the large-scale fluctuations of the interplanetary magnetic field strength observed in situ by both *Voyager 1* and *2* spacecraft (Macek et al. 2011, 2012). These observations are from the magnetic field experiment on the Voyager spacecraft (PI: N. F. Ness), which are reported by Behannon et al. (1977). We have studied these data in the deep heliosphere and after crossing the heliospheric termination shock in 2004 and 2007, respectively, i.e., in the heliosheath, and even now ahead of the heliopause, which is the last boundary separating the heliospheric plasma from the interstellar medium. Using a simple pressure balance the distance from the Sun to the heliospheric boundary was estimated to be ≈120 AU (Macek 1998).

The multifractal structure in the large-scale fluctuations in the solar wind magnetized plasma was made evident by Burlaga (1991). Early work on this subject and its relationship to turbulence was summarized by Burlaga (1995). To better understand scaling of solar wind turbulence, Macek (2007) and Macek & Szczepaniak (2008) have proposed a generalized one-dimensional model based on the Cantor set with two scaling and one weight parameters. A similar model was introduced by Burlaga et al. (1993) to describe multifractal spectra of magnetic field fluctuations in the heliosphere. Using this phenomenological model, we have shown that this complex nonlinear solar system may exhibit multifractal scaling. We have investigated the multifractal spectrum and showed that our model can explain the observed asymmetric spectrum in the heliosphere (Macek & Wawrzaszek 2009), in contrast to the nearly symmetric spectrum in the heliosheath (Burlaga et al. 2006; Burlaga & Ness 2010; Macek et al. 2011). We have identified the change of the asymmetry of the spectrum at the

termination shock, the slow decrease of the multifractality with the distance from the Sun and its modulation by the phases of the solar cycle, resulting in the evolution of the solar system plasma (Macek et al. 2011, 2012).

In this paper we extend our analysis further in the entire heliosheath and even when crossing the heliopause in 2012. We show that our phenomenological multifractal model of intermittent turbulence in space plasmas exhibits some typical properties that could shed light on universal characteristics of turbulence.

2. Fractals and Multifractals

The basic concepts of fractal sets are elucidated in textbooks (e.g., Falconer 1990; Ott 1993). We only note here that fractals are characterized by *self-similarity*, which is described by a single fractal dimension (independent of scale). On the other hand, a multifractal is a more complex object that exhibits different self-similarities (dependent on scale), which is described by the spectrum of dimensions or a multifractal singularity spectrum.

2.1. Multifractal Characteristics

A comparison of the main characteristics of fractals (with a usual measure of the volume of a set) and multifractals (with a probability measure to visit a fraction of the set) are summarized below.

Fractal	Multifractal
A volume V of a set as a function of size l	A probability versus singularity strength, α
$V(l) \sim l^{D_{\rm F}}$	$p_i(l) \propto l^{\alpha_i}$
A number of elements of size l needed to cover the set	A number of necessary elements in a range $(\alpha, \alpha + {\rm d}\alpha)$
$N(l) \sim l^{-D_{\rm F}}$	$N_l(\alpha) \sim l^{-f(\alpha)}$
The fractal dimension	The multifractal singularity spectrum
$D_{\rm F} = \lim\limits_{l\to 0} \dfrac{\ln N(l)}{\ln 1/l}$	$f(\alpha) = \lim\limits_{\varepsilon\to 0} \lim\limits_{l\to 0} \dfrac{\ln[N_l(\alpha+\varepsilon) - N_l(\alpha-\varepsilon)]}{\ln 1/l}$

The generalized dimension

$$D_q = \frac{1}{q-1} \lim_{l\to 0} \frac{\ln \sum_{i=1}^{N} (p_i)^q}{\ln l}$$

We should note that the generalized dimensions D_q could be nonlinear functions of any real index q, and this gives us important information about multifractality of the considered system (Ott 1993). In an equivalent way, one can use the singularity spectra $f(\alpha)$ versus a singularity strength α, which also characterize multifractality of the system under study (Falconer 1990). This is the method used by Burlaga (1995) to describe multifractal fluctuations. The two values of α at which $f(\alpha) = 0$ describe the character of the multifractal spectrum. Generally, with the *Voyager* observations, one can only determine the points near the maximum of $f(\alpha)$. One can either 1) extrapolate these points to determine the two intercepts to where $f = 0$ using a cubic (asymmetric) or parabolic (symmetric) distribution or 2) fit the observations with a model such as the p-model for

symmetric distributions or a two-scale model, such as that used by Burlaga et al. (1993), or Macek & Wawrzaszek (2009). These functions illustrated in Figure 4 of Wawrzaszek & Macek (2010), as thoroughly discussed by Macek (2012), allow a comparison of the experimental results with the phenomenological models of turbulence (Frisch 1995).

In addition to a usual probability measure $p_i(l)$ associated with a given scale l, we can replace the probability measure by so-called pseudoprobability measures

$$\mu_i(q,l) \equiv \frac{p_i^q(l)}{\sum_{i=1}^{N} p_i^q(l)}. \tag{1}$$

For a given q, using a fractal dimension index $f_i(q,l) \equiv \log \mu_i(q,l)/\log l$, the multifractal spectrum can be directly calculated as the average using the pseudoprobability measure $\mu_i(q,l)$ in Equation (1) indicated by the angled brackets $\langle \cdots \rangle$ (Chhabra & Jensen 1989)

$$f(q) \;\equiv\; \lim_{l\to 0} \sum_{i=1}^{N} \mu_i(q,l)\; f_i(q,l) = \lim_{l\to 0} \;\frac{\langle \log \mu_i(q,l) \rangle}{\log(l)}. \tag{2}$$

The corresponding average value of the singularity strength is given by Chhabra et al. (1989)

$$\alpha(q) \;\equiv\; \lim_{l\to 0} \sum_{i=1}^{N} \mu_i(q,l)\; \alpha_i(l) = \lim_{l\to 0} \;\frac{\langle \log p_i(l) \rangle}{\log(l)}. \tag{3}$$

3. Multifractal Model

The generalized weighted Cantor set is a simple example of multifractals as explained, e.g., by Falconer (1990). This model is illustrated in Figure 2 of Macek (2007). Macek & Wawrzaszek (2009) have argued that it provides a useful tool for phenomenological analysis of complex turbulent media. Namely, when constructing this more complex Cantor set we specify two scales l_1 and l_2 ($l_1 + l_2 \leq 1$) associated with two respective probability measures p and $1 - p$.

The difference between the calculated maximum and minimum dimensions, related to the respective regions in the phase space with the least and most dense probability densities has been proposed by Macek (2007) and Macek & Wawrzaszek (2009)

$$\Delta \equiv \alpha_{\max} - \alpha_{\min} = D_{-\infty} - D_{\infty} = \left| \frac{\log(1-p)}{\log l_2} - \frac{\log(p)}{\log l_1} \right|, \tag{4}$$

as a degree of multifractality. Naturally, this parameter Δ exhibits a deviation from a strict self-similarity, and it can also be used as a degree of intermittency as explained in (Frisch 1995, chapter 8). In the solar wind it could reveal nonlinear pressure pulses related to magnetosonic waves (Burlaga et al. 2003, 2007). The next quantitative parameter, describing the nature of the multifractal scaling, is the measure of asymmetry of the spectrum defined by Macek & Wawrzaszek (2009)

$$A \equiv \frac{\alpha_0 - \alpha_{\min}}{\alpha_{\max} - \alpha_0}, \tag{5}$$

where $\alpha = \alpha_0$ is the point at which the spectrum has its maximum, $f(\alpha_0) = 1$. The case when $A = 1$ ($l_1 = l_2 = 0.5$) corresponds to the one-scale p-model (e.g., Meneveau & Sreenivasan 1987).

4. *Voyager* Data

The trajectories of the *Voyager 1* and *2* spacecraft are shown in Figure 1 of Macek et al. (2012). *Voyager 1* crossed the termination shock on December 2004 December 16 at 94 AU from the Sun. It has been suggested that that *Voyager 1* entered the interstellar plasma at 121.7 AU, when the galactic cosmic ray intensity increased on day 238 (August 25) 2012 (Webber & McDonald 2013), but without significant changes in the direction of the magnetic field across the particle boundaries (Burlaga et al. 2013b). However, the plasma wave observations show that *Voyager 1* has only been observing electron plasma oscillations from day 297 to day 332 in 2012 and another such event during 2013 (Gurnett

et al. 2013; Burlaga et al. 2013a). Burlaga & Ness (2014) present evidence that *Voyager 1* has measuring interstellar magnetic fields since 209 in 2012 (2012 July 27) after crossing a current sheet that may have been related to the heliopause, while *Voyager 2* is still in the heliosheath and is expected to cross the heliopause in several years. Here we only analyze data of the magnetic field strength acquired on board the *Voyager 1* spacecraft before ($\lesssim$94 AU) and after the shock crossing (2005–2012) at 95–122 AU, i.e., in the entire heliosheath. Therefore, this work is an important extension of our previous analysis (Macek et al. 2011). A separate analysis is required for the fluctuations in the magnetic field directions, especially when trying to explain why the directions measured by Voyager 1 on both sides of the heliopause are so similar (Opher & Drake 2013; Grygorczuk et al. 2014).

The generalized multifractal measures $p(l)$ depending on scale l can be constructed using magnetic field strength fluctuations in the following way (Burlaga 1995). Namely, first normalizing a time series of daily averages $B(t_i)$, where $i = 1, \ldots, N = 2^n$ for $j = 2^{n-k}$, $k = 0, 1, \ldots, n$

$$p(x_j, l) \equiv \frac{1}{N} \sum_{i=1+(j-1)\Delta t}^{j\Delta t} B(t_i) = p_j(l), \tag{6}$$

is calculated with the successive average values $\langle B(t_i, \Delta t)\rangle$ of $B(t_i)$ between t_i and $t_i + \Delta t$, for each $\Delta t = 2^k$ (Macek et al. 2011). Using Taylor's hypothesis, one can argue that $p(x_j, l)$ can be regarded as a probability that at a position $x = v_{\rm sw}t$, at time t, where $v_{\rm sw}$ is the average solar wind speed, a given magnetic flux is transferred to a spatial scale $l = v_{\rm sw}\Delta t$.

Burlaga (1995) has shown that in the inertial range the average value of the qth moment of B at various scales l should scale as

$$\langle B^q(l)\rangle \sim l^{\gamma(q)}, \tag{7}$$

where the exponent γ is related to the generalized dimension, $\gamma(q) = (q-1)(D_q - 1)$. Following this method, using these slopes for each real q, the values of D_q can be determined

(Equation (7)). Alternatively, as explained in Section 2, the multifractal function $f(\alpha)$ versus scaling index α, which exhibits universality of the multifractal scaling behavior, can be obtained using the Legendre transformation. It is worth noting, however, that we obtain this multifractal universal function directly from the slopes given in Equations (2) and (3), using this direct method in various situations (see, Macek & Wawrzaszek 2009; Macek et al. 2011, 2012).

5. Results

In Figures 1 and 2 both average logarithmic probability and pseudoprobability measures $\langle \log_{10} p_i(l) \rangle$ and $\langle \log_{10} \mu_i(q,l) \rangle$ versus $\log_{10} l$ are presented for the values of q: 6, 4, 2, 1, 0, -1, -2, as obtained using the *Voyager 1* data of the solar wind magnetic field strength fluctuations in the heliosheath in 2010–2012. Namely, in Figure 1 we see the slopes identified in the heliosheath in 2010 and 2011 at distances of 112–115 AU and 116–118 AU, respectively. However, in Figure 2 the results are shown for two periods: (a) and (c) for days 1–128 before arriving at the heliopause and (b) and (d) for days 250–313 (uniform scaling) after crossing the heliopause at 122 AU. It is important to underline that the nature of scaling is changing when entering the interstellar plasma.

We see that the calculated slopes can be fitted to straight lines in the range of timescales typically of 2–16 days. Hence we can calculate the multifractal spectrum and compare with our two-scale model and the one-scale p-model, as discussed in Section 3, with the model parameters fitted using the magnetic field data (Macek & Wawrzaszek 2009; Macek et al. 2012).

We calculate the multifractal parameter Δ, Equation (4), in the heliosheath depending on the heliospheric distances during different phases of the solar cycle: minimum (MIN),

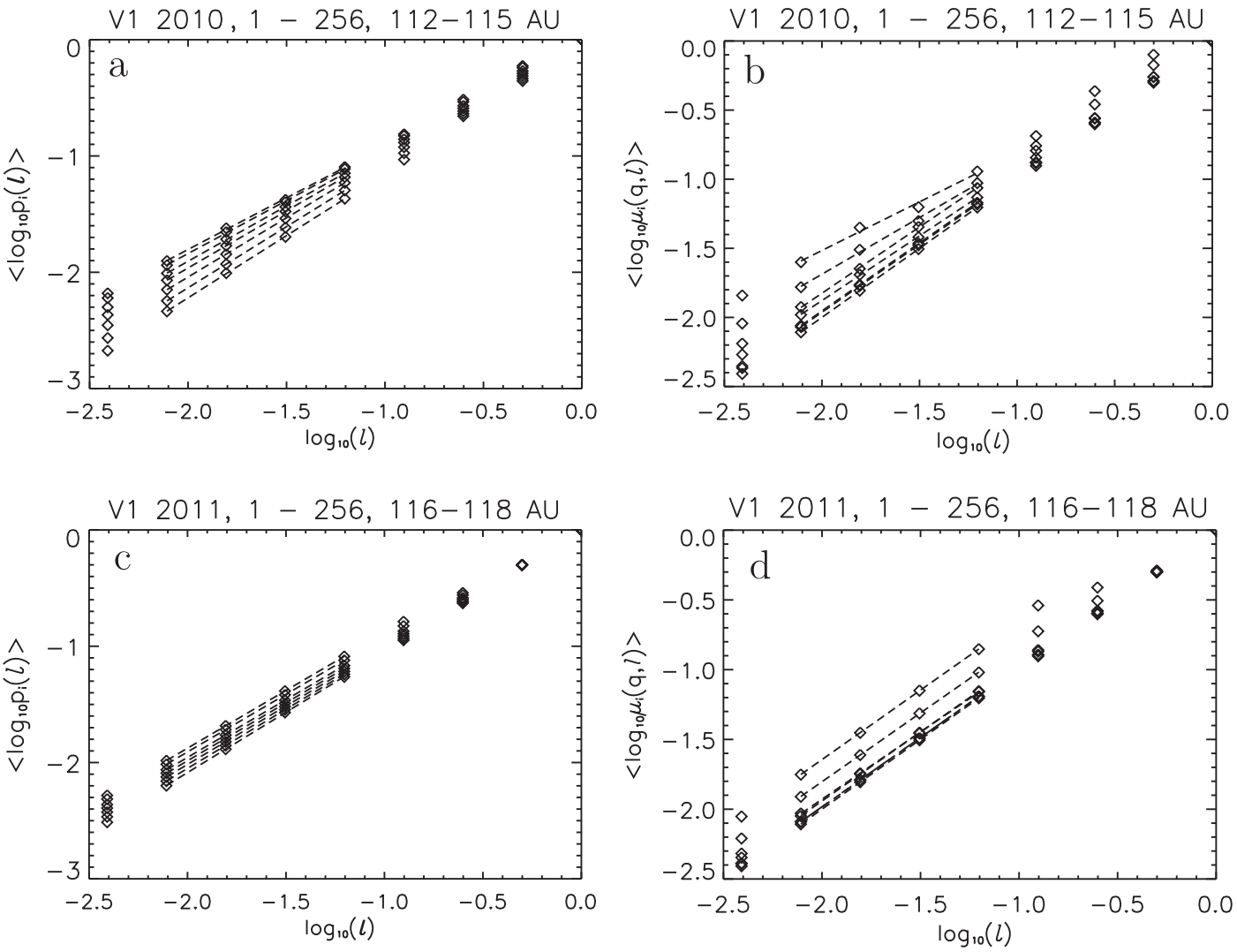

Fig. 1.— Generalized average logarithmic probability $\langle \log_{10} p_i(l) \rangle$ (a), (c) and pseudoprobability $\langle \log_{10} \mu_i(q,l) \rangle$ (b), (d) depending on $\log_{10} l$ for $-2 \le q \le 6$. These results are obtained using the magnetic field measurements of Voyager 1 in the heliosheath (shown by diamonds) in 2010 and 2011 at distances of 112–115 AU and 116–118 AU, respectively.

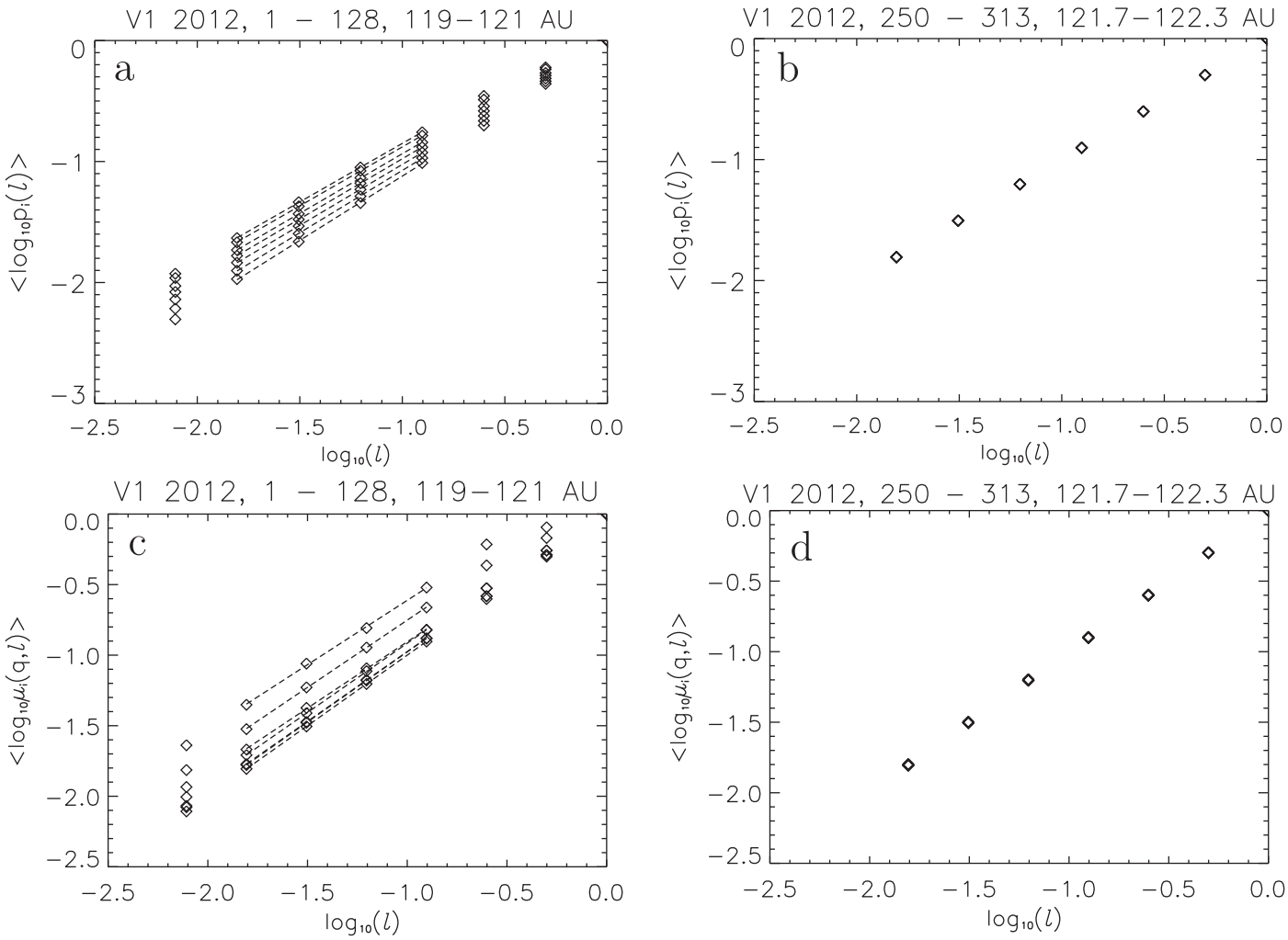

Fig. 2.— Generalized average logarithmic probability $\langle \log_{10} p_i(l) \rangle$ (a, b) and pseudoprobability $\langle \log_{10} \mu_i(q,l) \rangle$ (c, d) depending on $\log_{10} l$ for $-2 \leq q \leq 6$. These results are obtained using the *Voyager 1* magnetic field intensity measurements in the heliosheath before (a), (c) and after (b(, (d) crossing the heliopause (diamonds) at 122 AU.

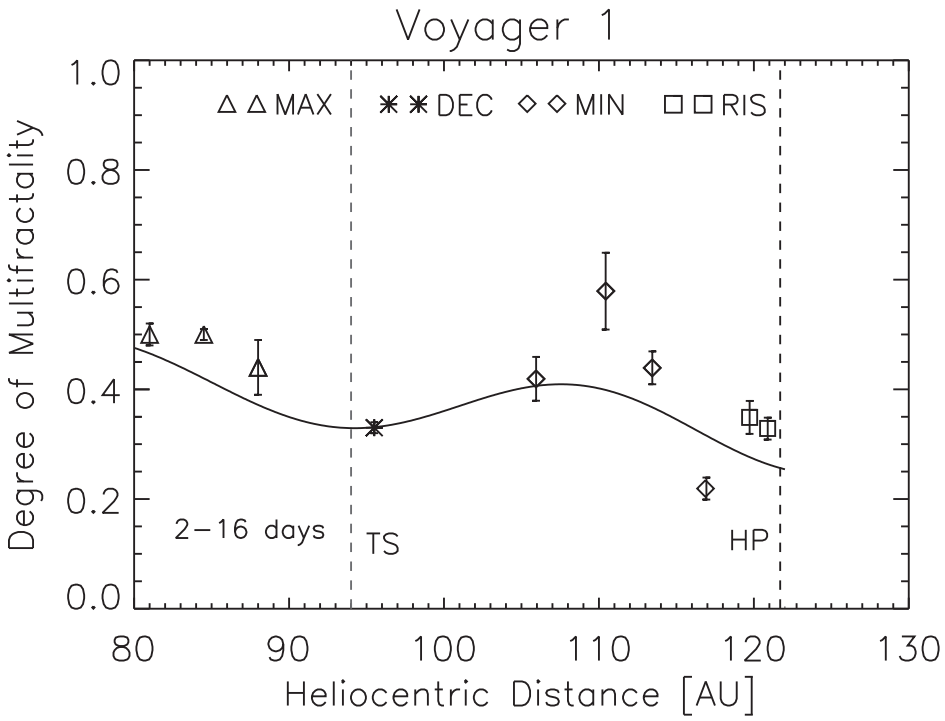

Fig. 3.— Parameter Δ quantifying multifractality in the heliosheath as a function of the distances from the Sun together with a periodic function shown by a continuous line during different phases of the solar cycle. The TS and the HP crossings by *Voyager 1* are also indicated.

maximum (MAX), declining (DEC) and rising (RIS) phases. The determined values of Δ are consistent with the fitted periodically decreasing function of time (in years) $20.27 - 0.00992t + 0.06\sin((t - 1980)/(2\pi(11)) + \pi/2)$, demonstrated in Figure 3 by a continuous line, as obtained by Macek et al. (2011). The crossings of the termination shock (TS) and the heliopause (HP) by *Voyager 1* are indicated by vertical dashed lines. The multifractality decreases slightly with distance and is still modulated depending on the phases of solar activity (Macek et al. 2011, 2012). Further in the heliosheath the degree of multifractality essentially still follows the periodic dependence fitted inside the heliosphere except a somewhat higher value of Δ obtained in 2009 near 110 AU. However, in this case because of sector boundary crossings we have used magnetic data exceptionally for days 43–299 in 2009 (instead of days 1–256) as used by Burlaga & Ness (2010).

The values of the parameter A describing the asymmetry of the multifractal spectrum, given in Equation (5), in the distant heliosphere during various phases of the solar cycles are shown in Figure 4; the value $A = 1$ for symmetric case (dotted) recovers the one-scale p model. Because the density of the probability measure $\varepsilon \propto l^{\alpha-1}$, this should correspond to the critical value where $\alpha = 1$, with roughly constant value of the probability measure density. In the heliosphere, one sees that there are no points above unity inside the heliosphere just before entering the heliosheath. We have already seen that a right-skewed spectrum is observed, $A < 1$, $\alpha > 1$, in the heliosphere (before the termination shock crossing; see Macek et al. (2011). However, it should be noted that Burlaga et al. (2006) found that a symmetric quadratic fit to the observations just before the termination shock provided a very good fit to the observed $f(\alpha)$. Generally, the analysis of the values of the parameter A presented in Figure 4 suggests that asymmetry is changing at the termination heliospheric shock. This can be explained by the change in the probability measure (ε) density of the magnetic field at the termination shock. Next, regardless of the rather large errors and limited samples, it would seem that a symmetric spectrum is preferred in the

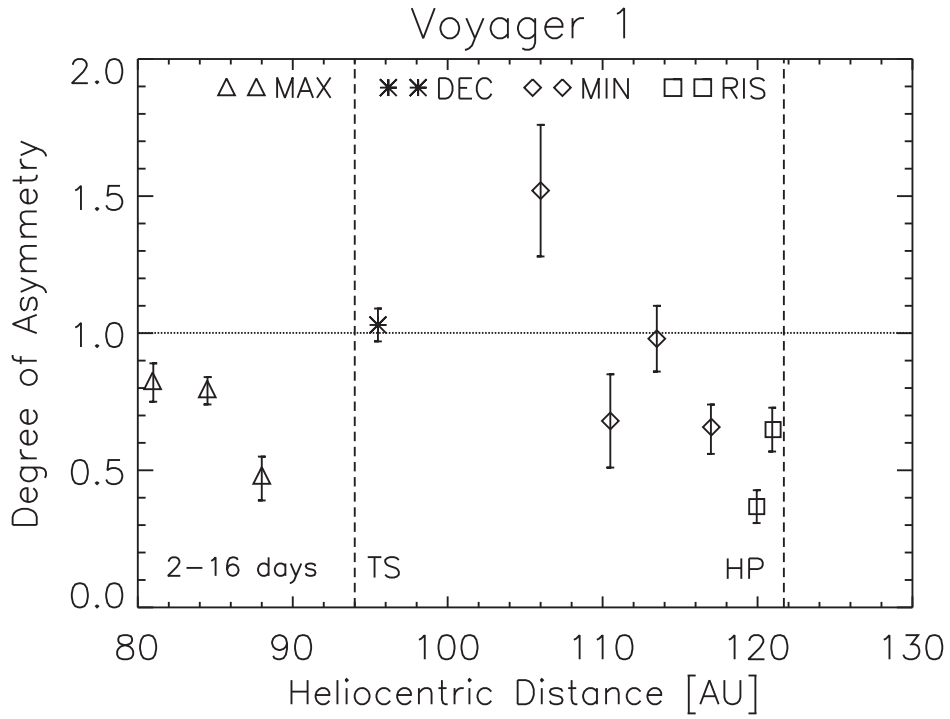

Fig. 4.— Parameter A describing the asymmetry of the spectrum in the heliosheath depending on the heliospheric distance during various phases of the solar cycles; the value $A = 1$ (dotted) recovers the one-scale model. The TS and the HP crossings by *Voyager 1* are also indicated.

Table 1: Values of Parameters Describing Multifractality Δ and Asymmetry A of the Spectra for the Magnetic Field Strength Identified by *Voyager 1* at Various Distances from the Sun, before and after Crossing the Termination Shock and at the Heliopause

Heliocentric Distance	**Year**	**Multifractality** Δ	**Asymmetry** A
$7-40$ AU	1980-1989	$0.55-0.73$	$0.47-1.39$
$40-60$ AU	1990-1995	$0.41-0.62$	$0.51-1.51$
$70-90$ AU	1999-2003	$0.44-0.50$	$0.47-0.96$
$95-107$ AU	2005-2008	$0.33-0.42$	$1.03-1.52$
$108-115$AU	2009-2010	$0.44-0.58$	$0.88-0.98$
117 AU	2011	0.22 ± 0.02	0.65 ± 0.09
120 AU	2012 (1–128)	0.35 ± 0.03	0.37 ± 0.06
121 AU	2012 (108–236)	0.33 ± 0.02	0.65 ± 0.08
122 AU	2012 (250–313)	–	–

heliosheath (Burlaga et al. 2006; Burlaga & Ness 2010; Macek et al. 2011), except for an asymmetric spectrum near 106 AU and around 120 AU. Note that another change in the asymmetry closer to the heliopause seems to be observed and the multifractal spectrum becomes more symmetric before crossing the heliopause.

The values of Δ and A computed by Burlaga et al. (2006) and Burlaga & Ness (2010) have been given in Table 1 of our previous paper (cf. Macek et al. 2011) for distances of 7–107 AU (1980–2008). The values calculated for the new range of distances of 108–122 AU (2009–2012) as seen in Figures 1 and 2 (except 2009) are now added in Table 1. Anyway, one sees that the parameters describing multifractality for the large-scale fluctuations of the interplanetary magnetic field resulting from independent analysis procedures are in

rather good agreement, possibly with the exception of a somewhat higher value of Δ near 110 AU (cf. Burlaga & Ness 2010, Figure 7). We have taken typical scaling range of 2–16 days, but we have also verified that the value of Δ is not very sensitive to the width of the inertial range; the scaling for 2–16 days, 2–32 days, and 4–32 days have been taken for calculations. In fact, the typical range of 2–16 days corresponds to the smallest deviation from the modulation curve in Figure 3.

We observe that the values of this multifractality parameter before the shock crossing, $\Delta = 0.4 - 0.7$, are slightly greater than those after shock crossing $\Delta = 0.3$–0.4. Burlaga et al. (2006) found symmetric spectrum with $\Delta = 0.65$ before the termination shock and 0.34 after the termination shock. Moreover, this results in a decrease in the intermittency exponent (Burlaga et al. 2006, Equation (5)) by a factor of 3.4, i.e., from 0.072 in the distant solar wind to 0.021 in the heliosheath, indicating that the heliosheath is significantly less intermittent than the distant solar wind. It is worth noting that similar values $\Delta = 0.35 \pm 0.03$ and $A = 0.37 \pm 0.06$ have been obtained for the first half 2012 (days 1–128) before the crossing of the heliopause; see Figure 2. For another period of that year (days 250–313), which does not include the shock in interstellar plasma (Burlaga et al. 2013b; Burlaga et al. 2013a), we no longer observe any multifractality. This means that after crossing the heliopause we might have non-intermittent behavior (the spectrum has formally reduced to one point, $\Delta = 0$), but we do not confirm any monofractal nature; this would certainly require further studies.

Finally, as suggested by Macek & Grzedzielski (1985), Fahr et al. (1986), and Macek (1989) reconnection may play an important role for the plasma transport across the heliopause. Recent studies by Swisdak et al. (2013) and simulations by Strumik et al. (2013, 2014) support this idea. Therefore, reconnection processes could modify fractal properties, but probably on smaller scales.

In summary, in this Letter we provide important evidence that the large-scale magnetic field fluctuations reveal the multifractal structure not only in the outer heliosphere, but in the entire heliosheath, even near the heliopause. Naturally, the evolution of the multifractal distributions should be related to some physical (MHD) models, as shown by Burlaga et al. (2003, 2007). The driver of the multifractality in the heliosheath could be the solar variability on scales from hours to days, fast and slow streams or shocks interactions, and other nonlinear structures discussed by Macek & Wawrzaszek (2013). In our view, any accurate physical model must reproduce the multifractal spectra. In particular, the observed non-multifractal scaling after the heliopause crossing suggest a non-intermittent behavior in the nearby interstellar medium, consistent with the smoothly varying interstellar magnetic field reported by Burlaga & Ness (2014).

6. Conclusions

We have identified the scaling region of fluctuations of the interplanetary magnetic field, Figures 1 and 2. In fact, using our two-scale model based on the weighted Cantor set, we have examined the universal multifractal spectra before and after *Voyager 1* crossed the termination shock at 94 AU and before the spacecraft crossed the heliopause at distances of about 122 AU from the Sun.

Moreover, inside the heliosphere we observe the asymmetric spectrum, which becomes more symmetric in the heliosheath. When approaching the heliopause, the deviation from symmetry decreases, and the spectrum seems to be rather symmetric close to the heliopause.

We confirm that the multifractality of magnetic field fluctuations embedded the solar wind plasma decreases slowly with the heliospheric distance, demonstrating in this Letter that this quantity is still modulated by the solar cycles further in the heliosheath, and

even in the vicinity of the heliopause, possibly approaching a uniform non-intermittent behavior in the nearby interstellar medium, which could be interesting for astrophysicists. We propose that this change in behavior is a signature of the expected crossing of the heliopause by *Voyager 2* in the near future.

W. M. Macek acknowledges participation in ISSI International Team 318. This work was supported by the European Community's Seventh Framework Programme ([FP7/2007–2013]) under Grant agreement No. 313038/STORM, and L. F. Burlaga was supported by NASA NNG14PN24P.

REFERENCES

Behannon, K. W., Acuña, M. H., Burlaga, L. F., et al. 1977, Space Sci. Rev., 21, 235

Burlaga, L. F. 1991, Geophys. Res. Lett., 18, 69

—. 1995, Interplanetary Magnetohydrodynamics (Oxford Univ. Press: New York)

Burlaga, L. F., F-Viñas, A., & Wang, C. 2007, J. Geophys. Res., 112, A7206

Burlaga, L. F., & Ness, N. F. 2010, Astrophys. J., 725, 1306

—. 2014, Astrophys. J., 784, 146

Burlaga, L. F., Ness, N. F., & Acuña, M. H. 2006, J. Geophys. Res., 111, A09112

Burlaga, L. F., Ness, N. F., Gurnett, D. A., & Kurth, W. S. 2013a, Astophys. J. Lett., 778, L3

Burlaga, L. F., Ness, N. F., & Stone, E. C. 2013b, Science, 341, 147

Burlaga, L. F., Perko, J., & Pirraglia, J. 1993, Astrophys. J., 407, 347

Burlaga, L. F., Wang, C., & Ness, N. F. 2003, Geophys. Res. Lett., 30, 1543

Chhabra, A., & Jensen, R. V. 1989, Phys. Rev. Lett., 62, 1327

Chhabra, A. B., Meneveau, C., Jensen, R. V., & Sreenivasan, K. R. 1989, Phys. Rev. A, 40, 5284

Fahr, H. J., Neutsch, W., Grzedzielski, S., Macek, W., & Ratkiewicz-Landowska, R. 1986, Space Sci. Rev., 43, 329

Falconer, K. 1990, Fractal Geometry: Mathematical Foundations and Applications (J. Wiley: New York)

Frisch, U. 1995, Turbulence. The Legacy of A.N. Kolmogorov (Cambridge Univ. Press: Cambridge)

Grygorczuk, J., Czechowski, A., & Grzedzielski, S. 2014, Astrophys. J. Lett., 789, L43

Gurnett, D. A., Kurth, W. S., Burlaga, L. F., & Ness, N. F. 2013, Science, 341, 1489

Macek, W. M. 1989, Adv. Space Res., 9, 257

Macek, W. M., & Grzedzielski, S. 1985, in Twenty Years of Plasma Physics, ed. B. McNamara (World Scientific: Singapure), 320–327

Macek, W. M. 1998, Highlights of Astronomy, 11B

—. 2007, Nonlinear Processes Geophys., 14, 695

Macek, W. M. 2012, in Exploring the Solar Wind, ed. M. Lazar (Intech: Croatia), 143–168

Macek, W. M., & Szczepaniak, A. 2008, Geophys. Res. Lett., 35, L02108

Macek, W. M., & Wawrzaszek, A. 2009, J. Geophys. Res., 114, A03108

Macek, W. M., & Wawrzaszek, A. 2013, Nonlinear Processes Geophys., 20, 1061

Macek, W. M., Wawrzaszek, A., & Carbone, V. 2011, Geophys. Res. Lett., 38, L19103

—. 2012, J. Geophys. Res., 117, A12101

Meneveau, C., & Sreenivasan, K. R. 1987, Phys. Rev. Lett., 59, 1424

Opher, M., & Drake, J. F. 2013, Astrophys. J. Lett., 778, L26

Ott, E. 1993, Chaos in Dynamical Systems (Cambridge Univ. Press: Cambridge)

Strumik, M., Czechowski, A., Grzedzielski, S., Macek, W. M., & Ratkiewicz, R. 2013, Astrophys. J. Lett., 773, L23

Strumik, M., Grzedzielski, S., Czechowski, A., Macek, W. M., & Ratkiewicz, R. 2014, Astrophys. J. Lett., 782, L7

Swisdak, M., Drake, J. F., & Opher, M. 2013, Astrophys. J. Lett., 774, L8

Wawrzaszek, A., & Macek, W. M. 2010, J. Geophys. Res., 115, A07104

Webber, W. R., & McDonald, F. B. 2013, Geophys. Res. Lett., 40, 1665

This manuscript was prepared with the AAS LaTeX macros v5.2.